

Self-Assembly

One-Dimensional Looped Chain and Two-Dimensional Square Grid Coordination Polymers: Encapsulation of Bis(1,2,4-Triazole)-*trans*-cyclohexane into the VoidsNayarassery N. Adarsh,^[a] Marinela M. Dîrtu,^[a] Philippe Guionneau,^[b,c] Eamonn Devlin,^[d] Yiannis Sanakis,^[d] Judith A. K. Howard,^[c] Basab Chattopadhyay,^[e] and Yann Garcia*^[a]

Abstract: Two new coordination polymers [Cu(btzx)₂(MeOH)₂](NO₃)₂ (**1**) and [Cu(btrcy)₂(H₂O)₂](ClO₄)₂·btrcy (**2**) have been synthesized by reacting two bis-triazole/tetrazole-ligands namely *m*-xylylene-bis(tetrazole) (btzx) and bis(1,2,4-triazole)-*trans*-cyclohexane (btrcy) with Cu(NO₃)₂ and Cu(ClO₄)₂ respectively in a 1:3 metal/ligand ratio. These compounds are shown to form X-ray quality single-crystals under different conditions, and the

crystal structures have been determined by single-crystal X-ray diffraction (SXRD). The SXRD data analysis revealed that **1** and **2** are 1D looped chain and 2D-square grid coordination polymers, respectively. More interestingly, the 2D-square grid architecture in **2** acts as an excellent host for the large guest ligand molecule btrcy, which is encapsulated within the voids of the 2D coordination polymer.

Introduction

Coordination polymers (CPs) or metal-organic frameworks (MOFs) have attracted considerable attention in recent years due to their diverse pore sizes, shapes, topologies, and unprecedented internal surface areas that can be appropriate for intriguing applications.^[1] Recently two dimensional coordination polymers (2D CPs) become popular in material science, not only due to their rich synthetic chemistry, chemical flexibility and the presence of metal ions that enhance novel optical, magnetic and electrical properties, but also due to their interesting nano-structure (nanosheet) and the resultant applications.^[2] In fact these 2D materials are not much explored, despite of some examples where it showed remarkable applications in biomimetic enzymes,^[3] molecular sieves membranes,^[4] gas separation^[5] catalysis^[6] and photoluminescence.^[7] Recently we reported a 2D corrugated sheet coordination polymer derived from Fe^{II} and a tris-tetrazole ligand, which showed remarkable spin crossover phenomena^[8] in both bulk single crystals and in exfoliated nanosheets.^[9]

Notwithstanding of these pioneering examples, control over the synthesis and applications of 2D materials based on CPs still remains a significant research challenge. 2D CPs can be synthesized by spontaneous supramolecular assembly of metal ions and multi-dentate ligands such as for instance bis-carboxylate, bis-pyridyl and bis-azole. The final supramolecular topology is however highly controlled by several factors such as metal/ligand ratio, solvent of crystallization, nature of the ligand, and the oxidation states of metal centers.^[10] It is evident from various reports that the nature of ligand is of great importance for the creation of 2D CPs.^[11]

MOFs or CPs derived from azole ligands, so called metal-azole frameworks (MAFs), in particular bis-triazole/tetrazole ligands, are still poorly explored.^[12] As a part of our ongoing research on the synthesis of novel MAFs, we are fascinated in studying the supramolecular structural diversities of these coordination networks and their driving forces (e.g. H-bonding, anions, ligating topology, etc.) in relationship with their functional properties (e.g. spin- crossover behavior, sorption properties, etc.).^[13] We have previously reported remarkable three dimensional chains of nanoballs derived from Cu(BF₄)₂ and 2-(4*H*-1,2,4-triazol-4-yl)acetic acid. The crystal structure analysis revealed that the self-assembly of the C₃-symmetric, μ₃-O bridged triangular tricopper SBU is the main driving force for the formation of nanoballs with a void size of ca. 1 nm and total solvent accessible volume of 4477.5 Å³, which accounts for 48 % of the cell volume.^[13a] We have also described a novel chiral helicate, derived from a triazole-carboxylate ligand and CdCl₂,^[13b] and more recently an unprecedented single walled Cu^{II} metal organic nanotube able to entrap metallic mercury.^[14]

With the aim to obtain new porous 2D CPs, we explore two bis-azole ligands and their supramolecular assembly with Cu^{II}. Furthermore, such ligands might exhibit an inter network supramolecular recognition property, which, in turn, might

[a] *Institute of Condensed Matter and Nanosciences, Université catholique de Louvain, Place L. Pasteur 1, 1348 Louvain-la-Neuve, Belgium*
E-mail: yann.garcia@uclouvain.be
<https://ygarcia.homestead.com/>

[b] *CNRS, Univ. Bordeaux, ICMCB, UMR 5026, 87 avenue du Dr. A. Schweitzer, 33608 Pessac, France*

[c] *University of Durham, Department of Chemistry, South Road, Durham, DH1 3LE, UK*

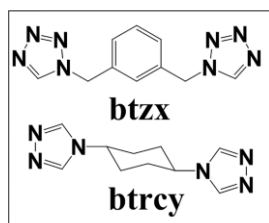
[d] *Institute of Nanoscience and Nanotechnology, NCSR Demokritos, Athens 15310, Greece*

[e] *Dr. Basab Chattopadhyay, Department of Physics, Norwegian University of Science and Technology (NTNU), Høgskoleringen, 7491 Trondheim, Norway*

Supporting information and ORCID(s) from the author(s) for this article are available on the WWW under <https://doi.org/10.1002/ejic.201801138>.

leads to the formation of more robust supramolecular host architectures and ensure guest encapsulation within the interstitial voids supported by intermolecular interactions.^[15,16] The integration of host molecules within the voids of the coordination cages, lead to the encapsulation of interesting molecules, extremely relevant to the development of useful chemotherapeutic drugs.^[17] The azole based ligand molecules attracted many researchers owing to their potential applications in medicinal chemistry.^[18]

Thus in order to obtain 2D CPs having encapsulated azole ligands, we deliberately reacted the rigid bis-1,2,4-triazole ligand **btrcy** and flexible bis-tetrazole ligand **btzx** with Cu^{II} [Cu(ClO₄)₂·6H₂O with **btrcy** and Cu(NO₃)₂·3H₂O with **btzx**] in 1:2 and 1:3 metal/ligand stoichiometric ratio (Scheme 1).



Scheme 1. Chemical structure of the azole ligands used in this work.

Results and Discussion

Synthesis and Spectroscopic Characterization

The **btzx** molecule was synthesized by following a previously reported procedure.^[19] Reaction of **btzx** with Cu(NO₃)₂·3H₂O in 1:3 or 1:2 metal/ligand ratio, separately in methanol solution lead to pale-green block shaped X-ray quality single crystals in

reasonable yield (53 %) of [Cu(**btzx**)₂(MeOH)₂](NO₃)₂ (**1**). The synthesis of **btrcy** was inspired from the patented procedure of Bayer et al.^[20] Reaction of **btrcy** with Cu(ClO₄)₂·6H₂O in water in a 1:3 ratio and 1:2 afforded a blue precipitate of [Cu(**btrcy**)₂(H₂O)₂](ClO₄)₂·**btrcy** (**2**) and [Cu(**btrcy**)₂(H₂O)₂](ClO₄)₂ (**3**), respectively. While the blue precipitate of **2** was recrystallized from water/acetone solution as dark blue colored single crystals under slow evaporation over a week time, **3** did not produce any crystals, under identical conditions. Attempts to recrystallize **3**, from different aqueous solution mixtures like water/methanol, water/ethanol, water/THF, water/1,4-dioxane, water/DMF, water/DMSO, were unsuccessful. Repeated synthesis with immediate filtration starting from a 1:2 ratio afforded a blue precipitate of [Cu(**btrcy**)₂(H₂O)₂](ClO₄)₂ (**3**). FT-IR spectra of **btzx** and **btrcy** contain characteristic bands at 3116 and 3124 cm⁻¹, corresponding to C–H fragments of the tetrazole and triazole groups, respectively. FT-IR spectra of **1** and **2** each contain a broad band for the water and methanol molecules centered at 3390–3400 cm⁻¹. A band for the tetrazole and triazole CH groups was found at 3122 and 3112 cm⁻¹ in the spectra of **1** and **2**, respectively. The nitrate counter anions were detected at 1382 cm⁻¹ in **1**.

Crystal Structures

Single crystal X-ray diffraction (SXRD) analysis of **1** revealed that it belongs to the triclinic *P* $\bar{1}$ space group (Table 1). The asymmetric unit comprises a Cu^{II}, one molecule of ligand **btzx** and methanol – both being coordinated to the Cu^{II} metal center and a nitrate counter anion. The Cu^{II} center displayed a slightly distorted square bipyramidal geometry [N–Cu–N = 88.89(7)–91.11(7)°, ∠N–Cu–O = 85.79(6)–94.21(6)°] (Table 2); the equatorial positions of the metal center are coordinated by tetrazole

Table 1. Crystal data.

Crystal data	1	2
Empirical formula	C ₂₂ H ₂₈ CuN ₁₈ O ₈	C ₁₅ H ₂₃ ClCu _{0.50} N ₉ O ₅
Formula weight	736.16	476.64
Crystal size [mm]	0.30 × 0.25 × 0.22	0.08 × 0.04 × 0.02
Crystal system	Triclinic	Triclinic
Space group	<i>P</i> $\bar{1}$	<i>P</i> $\bar{1}$
<i>a</i> [Å]	8.6210(18)	6.5086(4)
<i>b</i> [Å]	10.0631(17)	12.4962(8)
<i>c</i> [Å]	10.2123(11)	12.9374(8)
α [°]	81.089(12)	102.423(3)
β [°]	71.498(14)	94.894(3)
γ [°]	65.929(18)	92.474(3)
Volume [Å ³]	766.8(2)	1021.80(11)
<i>Z</i>	1	2
<i>D</i> _{calcd.} [g/cm ³]	1.594	1.549
<i>F</i> (000)	379	495
μ Mo- <i>K</i> α [mm ⁻¹]	0.791	0.743
<i>T</i> [K]	150(2)	293(2)
Range of <i>h, k, l</i>	–10/10, –12/12, –12/12	8/–9, 15/–17, 18/–18
θ min/max	2.92/25.99	1.619/30.371
Reflections collected/unique/observed	8369/2966/2859	8296/5363/3674
Data/restraints/parameters	2966/0/225	5363/0/313
Goodness of fit on <i>F</i> ²	1.066	1.020
Final <i>R</i> indices [<i>I</i> > 2 σ (<i>I</i>)]	<i>R</i> ₁ = 0.0323, <i>wR</i> ₂ = 0.0763	<i>R</i> ₁ = 0.0621, <i>wR</i> ₂ = 0.1275
<i>R</i> indices (all data)	<i>R</i> ₁ = 0.0342, <i>wR</i> ₂ = 0.0776	<i>R</i> ₁ = 0.1039, <i>wR</i> ₂ = 0.1481

N atoms and the apical positions are occupied by a methanol molecule. The extended coordination of the bis-tetrazole ligand (btzx) leads to the formation of a 1D looped chain coordination polymer (Figure 1a). The polymeric chains recognize the counter anion via O–H...O hydrogen bonding involving the metal bound methanol molecule and the counter anion nitrate [O...O = 2.696(5) Å; ∠O–H...O = 172.52°] (Figure 1a). Such chains are packed on top of each other in a slightly off-set fashion

Table 2. Selected bond lengths and bond angles associated with the coordination spheres of **1** and **2**.

Bond length [Å]	Bond length [Å]	Bond angle [°]	Bond angle [°]
1			
Cu(1)–N(2)	2.0308(16)	N(2)–Cu(1)–N(2)	180.02
Cu(1)–N(18)	2.0659(17)	N(2)–Cu(1)–N(18)	91.11(7)
Cu(1)–O(32)	2.2535(14)	N(2)–Cu(1)–N(18)	88.89(7)
		N(18)–Cu(1)–N(18)	179.998(2)
		N(2)–Cu(1)–O(32)	93.66(6)
		N(2)–Cu(1)–O(32)	86.34(6)
		N(18)–Cu(1)–O(32)	85.79(6)
		N(18)–Cu(1)–O(32)	94.21(6)
2			
Cu(1)–N(1)	2.036(2)	N(1)–Cu(1)–O(1)	91.53(11)
Cu(1)–N(4)	2.013(2)	N(1)–Cu(1)–O(1)	88.47(11)
Cu(1)–O(1)	2.432(3)	N(4)–Cu(1)–N(1)	90.56(10)
		N(4)–Cu(1)–N(1)	89.44(10)
		N(4)–Cu(1)–O(1)	85.17(11)
		N(4)–Cu(1)–O(1)	94.83(11)
		O(1)–Cu(1)–O(1)	180.02
		N(4)–Cu(1)–N(4)	180.02
		N(1)–Cu(1)–N(1)	180.02

sustained by various intermolecular interactions (Figure 1b). It is revealed from the overall packing of the looped chains along the crystallographic axis “a” that the template effect of the nitrate anion is one of the crucial factors for the formation of such chains in **1** (Figure 1c).

Compound **2** also crystallizes in the centrosymmetric triclinic space group $P\bar{1}$ (Table 1). The asymmetric unit (Figure 2a) contains one perchlorate anion, one ligand molecule (btzcy) centered on the $(\frac{1}{2}, \frac{1}{2}, \frac{1}{2})$ site and one Cu^{II} ion situated at the crystallographic cell origin and bonded to two ligands moieties and a water molecule. Each entity is generated in its entirety by the corresponding inversion centers. The unit cell content is Cu(C₁₀H₁₄N₆)₂(H₂O)₂·2(ClO₄)·C₁₀H₁₄N₆. Thus, each Cu^{II} ion which is linked to four ligands and two water molecules (Figure 2b) is surrounded by four N and two O atoms. Such a coordination environment of the Cu^{II} adopts the shape of a square bipyramid geometry which is defined by only two Cu–N distinct bond lengths [Cu–N4 = 2.014(2) Å and Cu–N1 = 2.035(2) Å], one Cu–O bond length [Cu–O1 = 2.431(3) Å] and the corresponding angles [N4–Cu–N1 = 89.42(9)°, N4–Cu–O1 = 85.20(10)° and N1–Cu–O1 = 91.53(11)] (Table 2). The Cu^{II} atoms are bridged by the ligands creating a polymeric structure in a two dimensional network (Figure 2b). The boughs formed by the ligands which link the copper atoms within a same layer are parallel to the [110] or to the [101] directions so as the 2D sheets are parallel to the (–111) crystallographic plane (Figure 2c). As a result, the shortest Cu...Cu separations do not bring into play copper atoms from a same layer: the interlayer Cu...Cu shortest separations correspond to the *a* [6.5086(4) Å], *b* [12.4962(8) Å] and *c* [12.9374(8) Å] cell parameters and the intra-layer Cu–Cu short-

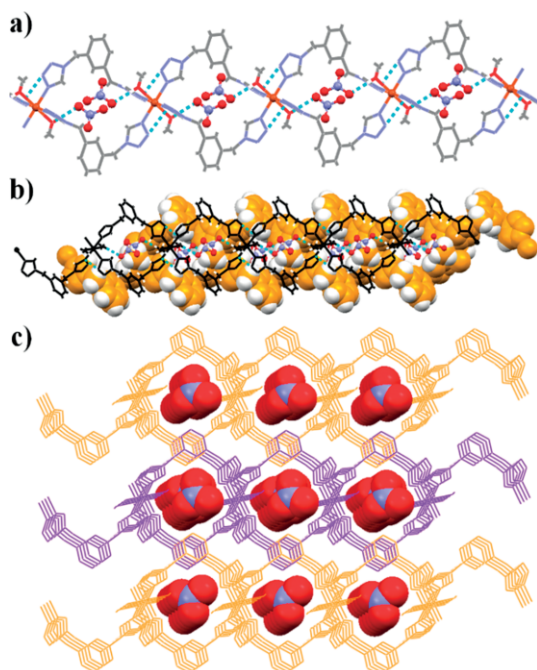


Figure 1. Crystal structure illustration of **1**; a) the looped chain CP in **1**; the hydrogen bonding interaction involving the nitrate anion and metal bound MeOH also displayed; b) offset packing of the looped chains supported by various hydrogen bonding and other weak interactions; c) occlusion of nitrate anion within the cavities of the looped chain CP.

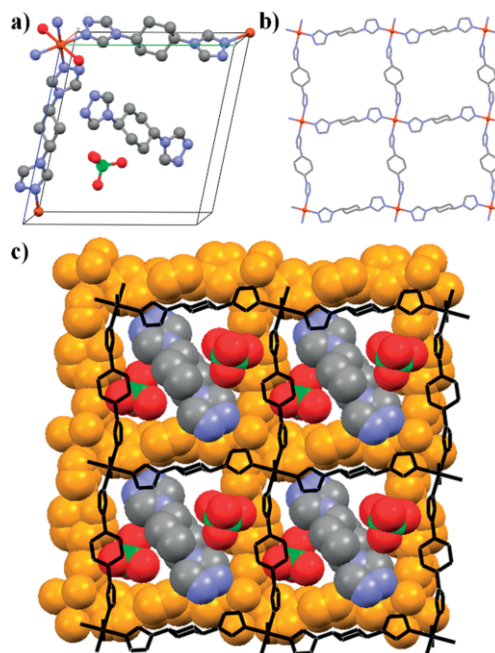


Figure 2. Crystal structure illustration of **2**; a) asymmetric unit of **2**; b) the square grid architecture in **2**; c) stacking modes of the square grids [adjacent grids are shown with orange (space-fill) and black (wireframe)]; occlusion of perchlorate anions and ligand molecules within the channels sustained by hydrogen bonding are also displayed.

est distances corresponds to the diagonal of the (ab) and (ac) planes [13.838(1) Å and 13.978(1) Å, respectively]. The average planes of the triazole entities from the same bough are all parallel for symmetrical reasons while the angle between the average plane of each triazole entity that belongs to a bough parallel to [101] and the average plane of a triazole entity that belongs to a bough parallel to [110] is 167.4(1)°. The sheets are stacked along the direction and are deduced from each other by a simple period translation, which results in the formation of real channels (Figure 2c). The shape of the section of such tubes is almost a square with a surface of around 195 Å².

These tubes can also be seen as infinite chains of cavities delimited by the ligands boughs, the volume of the cavities being, for symmetrical reasons, equal to the volume of the crystallographic cell (1022 Å³). Interestingly, one molecule of azole ligand and two perchlorate anions were encapsulated in these cavities (Figure 2c) supported by various H-bonding. The layers are linked to the guest molecules by H-bonding between the water molecules and the nitrogen atoms of the ligand [O1...N8 = 2.855(1) Å, H1A...N8 = 2.01(1) Å, O1-H1...N8 = 169(1)°] and between the ligands and the perchlorate anions [C2...O3 = 3.400(7) Å, H2...O3 = 2.527(5) Å, C2-H2...O3 = 157(1)°]. The perchlorate anions are also involved in H-bonding with the ligand molecules with the same cavity [C11-O5 = 3.370(5) Å, C11-H11...O5 = 169.8(3)°]. No relatively short distances are created between neighbouring cavity contents. The crystal structure of **2** differs from the crystal structures of two reported layered Cu^{II} based polymeric structure with bridging bis-triazole-alkane ligands.^[21] Indeed in the latter case the stacking mode prevents from the formation of channels within the crystals while in the present case such channels are generated and are filled with guest molecules and anions. Note that the crystal structure was also determined at 150 K but no changes were observed.

The Effect of Metal/Ligand Ratio on the Formation of 2D CPs

We studied the effect of metal/ligand stoichiometric ratio on the structure of Cu^{II} CPs derived from **btzx** and **btrcy**, in order to study the effect of metal/ligand ratio on the formation of 2DCPs. The reaction of **btzx** with Cu(NO₃)₂ in 1:2 and 1:3 exclusively resulted in pale blue single crystals (Figure 3b). FT-IR analysis of the blue single crystals obtained from each reaction revealed that both belong to 1D chain CP **1**; the FT-IR showed identical peaks: the band at 1378 cm⁻¹, attributed to the stretching N-O of the nitrate anion and the Figure print region of both samples showed identical peak position (Figure 3a). The scanning electron microscopy (SEM) image shown a fibrous morphology in these crystals (Figure 3c). Powder X-ray diffraction (PXRD) patterns of the crystalline products isolated from 1:2 and 1:3 stoichiometric experiments performed at the synthetic conditions of **1** match well with that of the simulated XRPD patterns obtained from the corresponding single crystal data, indicating the formation of **1**, irrespective to the metal/ligand ratio (Figure 3d).

In contrast to **1**, the starting reaction stoichiometry of 1:2 and 1:3 (metal/ligand) in synthesizing compound **2** turn out to

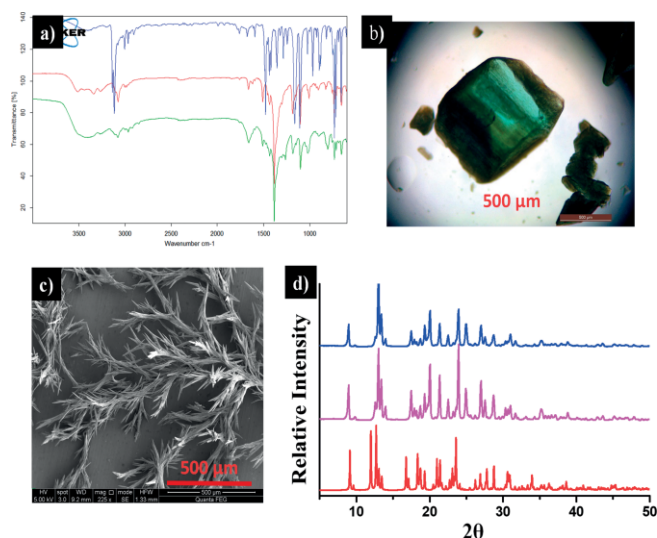


Figure 3. a) FT-IR comparison plot (blue: free ligand **btzx**; red and green: blue crystals obtained from 1:2 and 1:3 metal salt/**btzx** stoichiometric ratio, respectively); b) the optical microscope image of **1**; c) FE-SEM image of **1**; d) PXRD comparison plot under various conditions (red: simulated; magenta: obtained from 1:2 and 1:3 metal salt/**btzx** stoichiometric ratio, respectively).

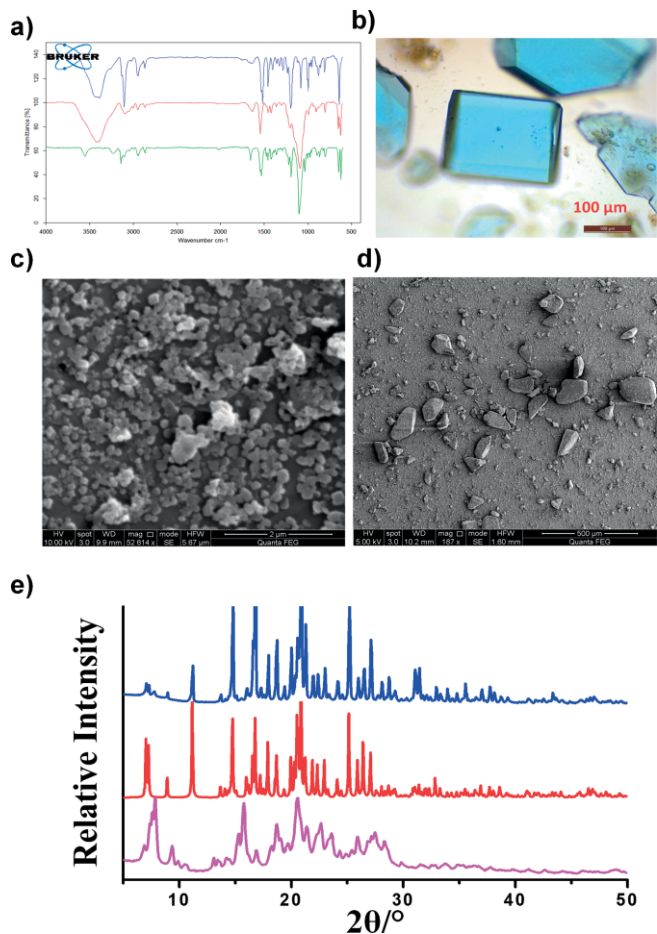


Figure 4. a) FT-IR comparison plot of **2**, **3** and **btrcy**; b) optical microscope image of crystals of **2**; c) and d) SEM image of **2** and **3**, respectively; e) PXRD comparison plot (blue: bulk crystals of **2**, red: simulated of **2**, magenta: bulk powder of **3**).

be two different crystalline phases. While the 1:2 metal/ligand ratio resulted in a microcrystalline blue powder, the 1:3 metal/ligand ratio lead to the formation of blue plate shaped single crystals (Figure 4b). FT-IR comparison plot confirmed that the blue powder and single crystals were chemically similar (with same functional groups and chemical entities) (Figure 4a). FT-IR spectra showed identical peaks: the band at 1258 cm^{-1} , attributed to the stretching N–O of the nitrate anion and the Figure print region of both samples showed identical peak positions (Figure 4a). Morphological characterization by FE-SEM revealed the presence of nanoparticles and block shaped crystals, from the products (blue powder and blue crystals) obtained from 1:2 and 1:3 (metal/ligand ratio), respectively (Figure 4c and 4d). Finally PXRD data confirmed that the microcrystalline blue powder and single crystals belong to two different crystalline phases (Figure 4e). While PXRD revealed that samples containing blue single crystals exhibit the same crystalline pattern that of the simulated pattern of **2** from the SXR data, the blue microcrystalline powder showed a different XRD pattern. Indexing of the powder diffraction pattern of this powder using the program DICVOL06^[22] showed triclinic unit cell having the cell parameters, $a = 13.36(1)$, $b = 13.97(2)$, $c = 13.35(2)$ Å; $\alpha = 62.38(1)$, $\beta = 98.2(1)$, $\gamma = 101.4(1)^\circ$; $V = 2159.14$ Å³, (Figure S1 in the Supporting Information). Thus from FT-IR, PXRD and SEM it is confirmed that the blue powder and single crystals obtained from the reaction of $\text{Cu}(\text{ClO}_4)_2$ and **btzcx** in 1:2 and 1:3 stoichiometric ratio, respectively are chemically identical, although their crystalline phases are different. Elemental analysis of blue powder and single crystals indicates the metal/ligand ratio of 1:2 and 1:3, respectively. Thus, we propose the formulation of the blue powder **3** as $[\text{Cu}(\text{btzcy})_2(\text{H}_2\text{O})_2](\text{ClO}_4)_2$.

Magnetic Studies

From the crystal structure, **1** can be considered as a 1D looped chain, in which Cu^{II} ions are linked by the large ligand **btzcx**. In Figure 5a we showed the temperature dependence of the magnetic susceptibility from a powder sample of **1**. At room temperature $\chi_M T = 0.47\text{ cm}^3\text{ mol}^{-1}\text{ K}$. This value is close to the value expected for an $S = 1/2$ system with $g > 2.0$. As the temperature decreases, $\chi_M T$ decreases slightly, reaching a value of $0.44\text{ cm}^3\text{ mol}^{-1}\text{ K}$ at 5 K. The temperature dependence of χ_M can be adequately modelled with the Curie law for an $S = 1/2$ system,

$$\chi_M = \frac{N\beta^2}{4kT} g^2$$

with $g = 2.16$, and including a Temperature Independent Paramagnetism (TIP) contribution of $9.8 \times 10^{-5}\text{ cm}^3\text{ mol}^{-1}$. The field dependence of magnetization at 5 K (inset of Figure 5a) follows the Brillouin function for an $S = 1/2$ system with $g = 2.16$ further indicating negligible intermolecular interactions. In Figure 5b we show the room temperature X-band EPR spectrum from a powdered sample of **1**. The spectrum is typical for an isolated Cu^{II} ion with axial properties ($g_{\parallel} > g_{\perp}$) and can be simulated with the spin Hamiltonian:

$$H = \beta \mathbf{B} \mathbf{g} \mathbf{S} + \mathbf{I} \mathbf{A} \mathbf{S}$$

where β is the Bohr magneton. The first term describes the Zeeman interaction and the second term the hyperfine interaction between the electronic $S = 1/2$ and the nuclear $I = 3/2$ spin of the $^{63/65}\text{Cu}$ nucleus. The spectra can be simulated with the following parameters: $g_{\parallel} = 2.31(1)$, $g_{\perp} = 2.08(1)$, $A_{\parallel} = 481(5)$ MHz, $A_{\perp} = 37(5)$ MHz. In order to account for the particular lineshape, a distribution on the \mathbf{g} -tensor components was used with $\sigma g_{\parallel} = 0.22$ and $\sigma g_{\perp} = 0.21$ and an intrinsic linewidth of 4.4 mT. From the determined \mathbf{g} -tensor components from the analysis of the EPR spectra the parameter

$$g = \frac{(g_{\parallel}^2 + 2g_{\perp}^2)^{1/2}}{3} = 2.16$$

is obtained which is in agreement with the g value determined from the magnetic susceptibility measurements. Overall, the combined magnetic measurements studies and EPR spectroscopic data for **1** are consistent with magnetically isolated Cu^{II} ions.

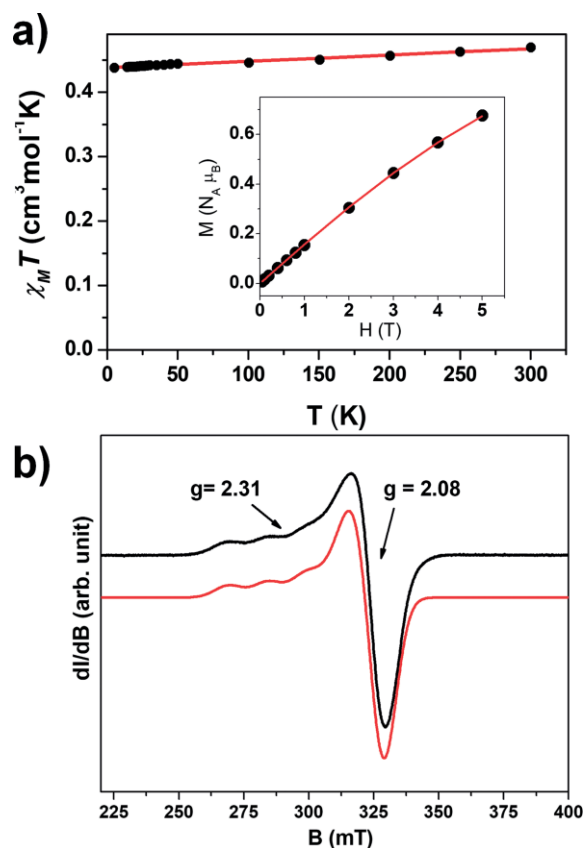


Figure 5. a) Temperature dependence of $\chi_M T$ in the presence of a magnetic field of 0.1 T from a powdered sample of **1**. Solid line is a simulation with the parameters shown in the text. Inset: The dependence of magnetization on the magnetic field at 5 K. b) Experimental (black line) and theoretical (red line) X-band EPR spectra from a powder sample of **1** at room temperature. EPR conditions: microwave power, 2.0 mW; modulation amplitude, 10 Gpp; microwave frequency, 9.42 GHz.

No magnetic studies were performed on the grids **2** and **3**, due to their expected paramagnetic behavior favored by long metal–metal distances (≈ 13.8 Å in **2**).

Conclusions

In summary, we have explored bis-azole based, ditopic ligands (**btzx** and **btrcy**) to search for a 2D CP having an octahedral metal center, and its capability for encapsulation of organic ligands. The tetrazole ligand **btzx** showed 1D CP structure in **1**, while polymerized with Cu^{II}. The NO₃⁻ anion acts as a template (the NO₃⁻ anion got entrapped within the cavity of the looped chain CP in **1**). On the other hand, the triazole ligand **btrcy** displays a 2D CP structure in CP **2**. Interestingly, the voids of the 2D square grid structure in **2** are used for the encapsulation of **btrcy** molecules and ClO₄⁻ anions, supported by hydrogen bonding interactions.

Experimental Section

Materials and Methods: All chemicals and solvents were commercially available (Aldrich) and used without further purification. The ligand *m*-xylylene-bis(tetrazole) (**btzx**) was synthesized by following a reported procedure.^[19] Elemental analysis was carried out at MEDAC (UK) and in Vernaison CNRS. FT-IR spectra were recorded on a Shimadzu Benelux FT-IR-84005 spectrometer using KBr discs at room temp. between 4000 and 400 cm⁻¹. Nuclear magnetic resonance (NMR) spectra were recorded on a Bruker ARX-250 spectrophotometer using [D₆]DMSO as solvent. FE-SEM images were performed on a scanning electron microscope (FEI Quanta 650 FEG) at acceleration voltages of 5–10 kV. Powder X-ray diffraction (PXRD) patterns were recorded on a PANalytical X'Pert PRO MRD (Cu-K_α radiation, λ = 1.5406 Å) X-ray diffractometer.

EPR: Room temperature X-band EPR spectra from a powdered sample of **1** were collected with an upgraded ER-200D Bruker EPR spectrometer, equipped with an Anritsu Frequency counter, and an NMR Gaussmeter.

Magnetism: Magnetic susceptibility measurements of **1** was performed on a MPMS-5500 Quantum Design instrument in the temperature range 5–300 K.

Caution: Perchlorate and tetrazole compounds are potentially explosive. Although no problem was encountered in the present study, care must be taken when handling such substances.

1,2-Bis(1,2,4-Triazol-4-yl)cyclohexane (btrcy): Freshly prepared anhydrous formic hydrazide (2.104 g, 0.03503 mol) and triethylorthoformate (6.97 mL, 0.0419 mol) in MeOH (40 mL) were heated to reflux for 2 h, then trans-cyclohexane diamine (2 g, 0.01752 mol) in anhydrous MeOH (15 mL) was added dropwise, and the mixture was kept at reflux for a further 6 h. After removal of the solvent under reduced pressure, a pale oily liquid obtained, which eventually solidified to a pinkish white residue. The residue formed was removed by filtration and recrystallized from MeOH (10 mL) to afford white crystalline material. Yield: 1.8 g (47 %). C₁₀H₁₄N₆ (218.26): calcd. C 55.03, H 6.47, N 38.50; found C 55.09, H 4.92, N 38.74. FT-IR (KBr): $\tilde{\nu}$ = 3444 (w), 3137 (m), 3107 (m), 3041 (w), 2965 (w), 1760 (s), 1703 (s), 1521 (m), 1441 (m), 1399 (s), 1365 (m), 1346 (s), 1186 (s), 1118 (m), 1075 (m), 1030 (m), 969 (m), 810 (w), 726 (m), 531 (m), 631 (m) cm⁻¹. ¹H NMR (300 MHz, [D₆]DMSO, 298 K): δ = 1.85–1.92 (t, J = 9.0 Hz, 4 H), 2.17–2.19 (d, J = 6.0 Hz, 4 H), 8.64 (s, 4 H) ppm. ¹³C NMR (300 MHz, [D₆]DMSO, 298 K): δ = 30.4, 34.8, 42.9, 123.6, 132, 134.5, 143, 168.5 ppm. HRMS: *m/z* calcd. for C₁₃H₁₃N₄O₂ [M + H⁺]: 218.13, found 218.12.

Synthesis of Coordination Polymers 1–3

[Cu(btzx)₂(MeOH)₂](NO₃)₂ (1) was synthesized by layering a methanolic solution of **btzx** (50 mg, 0.2064 mmol) over an aqueous solution of Cu(NO₃)₂·3H₂O (8.5 mg, 0.047 mmol) in water and future layering of a methanolic solution of Cu(NO₃)₂ (25 mg, 0.1032 mmol). The resultant bi-layer solution, thus obtained, was kept undisturbed. After two days, pale-blue block shaped X-ray quality crystals were obtained. Yield: 40 mg (53 %). C₂₂H₂₈CuN₁₈O₈ (736.12): calcd. C 35.90, H 3.83, N 34.25; found C 35.76, H 4.20, N 34.18. FT-IR (KBr): $\tilde{\nu}$ = 3466 (br. s, MeOH O–H stretch), 3091 (br. s, tetrazole C–H stretch), 3064 (w, aromatic C–H stretch), 1587 (s), 1548 (s), 1479 (s), 1429 (s), 1378 (s, nitrate N–O stretch), 1290 (s), 1246 (s), 1193 (m), 1168 (m), 1145 (m), 1128 (w), 1109 (w), 1082 (m), 964 (m), 931 (m), 810 (s), 731 (s), 719 (s), 694 (s), 665 (m), 648 (m), 605 (m), 594 (m), 578 (m) cm⁻¹.

[Cu(btrcy)₂(H₂O)₂](ClO₄)₂·btrcy (2): The **btrcy** molecule (0.19 g, 0.872 mmol) dissolved in hot water (20 mL) was added to a solution of [Cu(H₂O)₆](ClO₄)₂ (0.14 g, 0.291 mmol) in water (20 mL). The solution became turbid and a very fine blue precipitate appeared. The volume of the solution was completed to 210 mL with 10 mL of acetone and warmed to recrystallize the precipitate. The solution was left to evaporate for two months at room temperature, after which the volume of the solution was completed to 75 mL, and warmed to 100 °C. This last procedure did not dissolve the precipitate for which shining blue thin crystals were collected shortly afterwards. These crystals were washed with a minimum amount of water and dried in air. Yield: 20 mg (8 %). C₃₀H₄₆Cl₂CuN₁₈O₁₀ (953.26): calcd. C 37.8, H 4.86, N 26.45; found C 38.24, H 5.02, N 26.38. FT-IR (KBr): $\tilde{\nu}$ = 3442 (br. s, water O–H stretch), 3088 (br. s, triazole C–H stretch), 3062 (w, aromatic C–H stretch), 1502 (s), 1466 (s), 1418 (s), 1286 (s), 1232 (s), 1140 (m), 1122 (w), 1100 (w), 1072 (s, perchlorate Cl–O stretch), 961 (m), 822 (s), 723 (s), 666 (m), 628 (m), 601 (m), 504 (m) cm⁻¹.

[Cu(btrcy)₂(H₂O)₂](ClO₄)₂ (3): The **btrcy** molecule (0.19 g, 0.863 mmol) dissolved in hot water (20 mL) was added to a solution of [Cu(H₂O)₆](ClO₄)₂ (0.160 g, 0.432 mmol) in water (20 mL). A dark blue precipitate was obtained immediately, filtered, washed with water and air dried. Yield: 220 mg (69 %). C₂₀H₃₂Cl₂CuN₁₂O₁₀ (735.00): calcd. C 32.68, H 4.39, N 22.87; found C 33.12, H 5.04, N 23.06. FT-IR (KBr): $\tilde{\nu}$ = 3441 (br. s, water O–H stretch), 3078 (br. s, triazole C–H stretch), 3060 (w, aromatic C–H stretch), 1501 (s), 1469 (s), 1418 (s), 1286 (s), 1232 (s), 1141 (m), 1120 (w), 1101 (w), 1071 (s, perchlorate Cl–O stretch), 960 (m), 820 (s), 721 (s), 664 (m), 622 (m), 601 (m), 501 (m) cm⁻¹.

Single Crystal X-ray Diffraction Experiment: X-ray data collections of **1** were performed on a Mar345 image plate detector using Mo-K_α radiation (rotation anode, multilayer mirror) at 120(2) K. The data were integrated with the CrysAlisPro software.^[23] The implemented empirical absorption correction was applied. The structures were solved by direct methods using the SHELXS-97 program^[24] and refined by full-matrix least-squares on |F₂| using SHELXL-97.^[24] Non-hydrogen atoms were anisotropically refined and the hydrogen atoms were placed on calculated positions in riding mode with temperature factors fixed at 1.2 times U_{eq} of the parent atoms and 1.5 times U_{eq} for methyl groups.

Single crystals of **2** appear as intense blue regular spearheads. A small single crystal was mounted on a glass fiber and positioned on a Bruker smart CCD. After checking the quality of the diffraction pattern from preliminary scans, a data collection was run at room temperature. Considering the weakness of the Bragg peaks intensity the detector was positioned as close as possible from the sam-

ple (4.51 cm) and the time per frames was increased to 60 seconds. The diffraction frames were integrated using the SAINT package.^[25] The crystal structure was solved with both Patterson and direct methods and refined using SHELX-97 package^[24] in the Olex2 suite.^[26] The crystal structure was solved and refined in the non-centrosymmetric $P1$ (n°) and in the centrosymmetric $P\bar{1}$ (n°) space groups. Convergence is reached in both cases and final refinement reliability factors (R , wR) and other quality criteria [S , $(\Delta/\sigma)_{\max}$, σ] are close for the two solutions. Moreover, the differences between the lengths of the bonds in $P1$ which are equivalent by the center of inversion in $P\bar{1}$ appear to be quite small (< 0.1 Å). Nevertheless, anisotropic refinement of the thermal atom parameters in $P1$ provide anisotropic displacement ellipsoids slightly oblong for some atoms of the ligands which is not the case in $P\bar{1}$. In addition the C–C bond of the ligand molecule is found longer than usual values [C14–C15 = 1.61(1) Å] in $P1$ but not in $P\bar{1}$ [1.534(5) Å]. An exhaustive study of Pi – $P\bar{1}$ ambiguity by R. Marsh^[27] has pointed out that the centrosymmetric space group should be preferred if the $P1$ description leads to strange bond lengths which are improved in $P\bar{1}$, and the space group $P\bar{1}$ was definitely adopted. All non-hydrogen atoms were refined with anisotropic displacement parameters. All hydrogen atoms were located in difference Fourier maps and refined with constraints.

CCDC 1828697 (for **1**), and 1828038 (for **2**) contain the supplementary crystallographic data for this paper. These data can be obtained free of charge from The Cambridge Crystallographic Data Centre.

Supporting Information (see footnote on the first page of this article): Indexing data of **3** can be found in the Supporting information.

Acknowledgments

This work was supported by the Fonds National de la Recherche Scientifique-FNRS (PDR T.0102.15) and COST action CA15128. M. M. D. is a chargé de recherches from the F.R.S.-FNRS (Belgium). We thank the Belgian Science Policy and the Marie Curie Actions from the European Commission for a postdoctoral research fellowship allocated to N. N. A. E. D. and Y. S. acknowledge support by the project MIS 5002567, implemented under the “Action for the Strategic Development on the Research and Technological Sector”, funded by the Operational Programme “Competitiveness, Entrepreneurship and Innovation” (NSRF 2014–2020) and co-financed by Greece and the European Union (European Regional Development Fund).

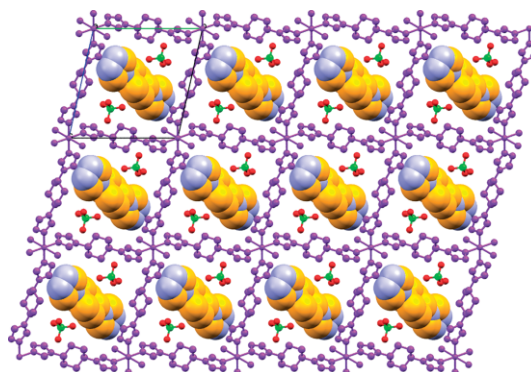
Keywords: Coordination polymers · N ligands · Host-guest systems · Structure elucidation

- [1] a) A. M. Spokoyin, D. Kim, A. Sumrein, C. A. Mirkin, *Chem. Soc. Rev.* **2009**, 38, 1218–1227; b) S. Kitagawa, S.-i. Noro, T. Nakamura, *Chem. Commun.* **2006**, 701–707; c) F. J. Muñoz-Lara, A. B. Gaspar, M. C. Muñoz, M. Arai, S. Kitagawa, M. Ohba, J. A. Real, *Chem. Eur. J.* **2012**, 18, 8013–8018; d) Y. Liao, S. K. Yang, K. Koh, A. J. Matzger, J. S. Biteen, *Nano Lett.* **2012**, 12, 3080–3085; e) S. Xiang, Y. He, Z. Zhang, H. Wu, W. Zhou, R. Krishna, B. Chen, *Nat. Commun.* **2012**, 3, 1956–1959; f) J. J. Gassensmith, H. Furukawa, R. A. Smaldone, R. S. Forgan, Y. Y. Botros, O. M. Yaghi, J. F. Stoddart, *J. Am. Chem. Soc.* **2011**, 133, 15312–15315; g) N. N. Adarsh, P. Dastidar, *Chem. Soc. Rev.* **2012**, 41, 3039–3060.
- [2] a) T. Rodenas, I. Luz, G. Prieto, B. Seoane, H. Miro, A. Corma, F. Kapteijn, F. X. Llabrés i Xamena, J. Gascon, *Nat. Mater.* **2015**, 14, 48–55; b) M. Zhao, Y. Huang, Y. Peng, Z. Huang, Q. Ma, H. Zhang, *Chem. Soc. Rev.* **2018**, 47, 6267–6295.
- [3] Y. Wang, M. Zhao, J. Ping, B. Chen, X. Cao, Y. Huang, Ch. Tan, Q. Ma, Sh. Wu, Y. Yu, Q. Lu, J. Chen, W. Zhao, Y. Ying, H. Zhang, *Adv. Funct. Mater.* **2016**, 28, 4149.
- [4] Y. Peng, Y. Li, Y. Ban, H. Jin, W. Jiao, X. Liu, W. Yang, *Science* **2014**, 346, 1356–1359.
- [5] Y. Zhang, X. Feng, S. Yuan, J. Zhou, B. Wang, *Inorg. Chem. Front.* **2016**, 3, 896–909.
- [6] a) G. Zhan, H. Chun Zeng, *Adv. Funct. Mater.* **2016**, 26, 3268–3281; b) R. Dong, M. Pfeiffermann, H. Liang, Z. Zheng, X. Zhu, J. Zhang, X. Feng, *Angew. Chem. Int. Ed.* **2015**, 54, 12058–12063; *Angew. Chem.* **2015**, 127, 12226–1223.
- [7] a) C. Hermosa, B. R. Horrocks, J. I. Martínez, F. Liscio, J. Gómez-Herrero, F. Zamora, *Chem. Sci.* **2015**, 6, 2553–2558; b) T. Araki, A. Kondo, K. Maeda, *Chem. Commun.* **2013**, 49, 552.
- [8] Y. Garcia, N. N. Adarsh, A. D. Naik, *Chimia* **2013**, 67, 411–418.
- [9] S. Suarez-Garcia, N. N. Adarsh, G. Molnár, A. Bousseksou, Y. Garcia, M. M. Dirtu, J. Saiz-Poseu, R. Robles, P. Ordejón, D. Ruiz-Molina, *ACS Appl. Mater. Interfaces* **2018**, 1, 2662–2668.
- [10] a) S. Kitagawa, R. Kitaura, S.-i. Noro, *Angew. Chem. Int. Ed.* **2004**, 43, 2334–2430; *Angew. Chem.* **2004**, 116, 2388; b) N. N. Adarsh, F. Novio, D. Ruiz-Molina, *Dalton Trans.* **2016**, 45, 11233–11255.
- [11] F. A. A. Paz, J. Klinowski, S. M. F. Vilela, J. P. C. Tomé, J. A. S. Cavaleiro, J. Rocha, *Chem. Soc. Rev.* **2012**, 41, 1088.
- [12] a) A. D. Naik, M. M. Dirtu, A. P. Railliet, J. Marchand-Brynaert, Y. Garcia, *Polymer* **2011**, 3, 1750; b) J.-P. Zhang, Y.-B. Zhang, J.-B. Lin, X.-M. Chen, *Chem. Rev.* **2012**, 112, 1001.
- [13] a) A. D. Naik, M. M. Dirtu, A. Léonard, B. Tinant, J. Marchand-Brynaert, B.-L. Su, Y. Garcia, *Cryst. Growth Des.* **2010**, 10, 1798; b) M. M. Dirtu, C. Neuhausen, A. D. Naik, A. Léonard, F. Robert, J. Marchand-Brynaert, B.-L. Su, Y. Garcia, *Cryst. Growth Des.* **2011**, 11, 1375; c) A. D. Naik, B. Tinant, A. Léonard, J. Marchand-Brynaert, B.-L. Su, Y. Garcia, *Cryst. Growth Des.* **2011**, 11, 4034; d) A. D. Naik, J. Beck, M. M. Dirtu, C. Bebrone, B. Tinant, K. Robeyns, J. Marchand-Brynaert, Y. Garcia, *Inorg. Chim. Acta* **2011**, 368, 21; e) Y. Garcia, F. Robert, A. D. Naik, G. Zhou, B. Tinant, K. Robeyns, S. Michotte, L. Piroux, *J. Am. Chem. Soc.* **2011**, 133, 15850; f) Y. Boland, B. Tinant, D. A. Safin, J. Marchand-Brynaert, R. Clérac, Y. Garcia, *CrystEngComm* **2012**, 14, 8153–8155; g) M. M. Dirtu, Y. Boland, D. Gillard, B. Tinant, K. Robeyns, D. A. Safin, E. Devlin, I. Sanakis, Y. Garcia, *Int. J. Mol. Sci.* **2013**, 14, 23597–23613.
- [14] N. N. Adarsh, M. M. Dirtu, A. D. Naik, A. F. Léonard, N. Campagnol, K. Robeyns, J. Snauwaert, J. Franssaer, B. L. Su, Y. Garcia, *Chem. Eur. J.* **2015**, 21, 4300–4307.
- [15] N. N. Adarsh, D. A. Tocher, J. Ribas, P. Dastidar, *New J. Chem.* **2010**, 34, 2458–2469.
- [16] Y. Jia, B. Wei, R. Duan, Y. Zhang, B. Wang, A. Hakeem, N. Liu, X. Ou, S. Xu, Z. Chen, X. Lou, F. Xia, *Sci. Rep.* **2014**, 4, 5929. <https://doi.org/10.1038/srep05929>.
- [17] Y.-R. Zheng, K. Suntharalingam, T. C. Johnstone, S. J. Lippard, *Chem. Sci.* **2015**, 6, 1189–1193.
- [18] a) N. Mast, W. Zheng, C. D. Stout, I. A. Pikuleva, *Mol. Pharmacol.* **2013**, 84, 86–94; b) K. Shalini, N. Kumar, S. Drabu, P. K. Sharma, *Beilstein J. Org. Chem.* **2011**, 7, 668–677.
- [19] M. Quesada, F. Prins, E. Bill, H. Kooiman, P. Gamez, O. Roubeau, A. L. Spek, J. G. Haasnoot, J. Reedijk, *Chem. Eur. J.* **2008**, 14, 8486.
- [20] H. O. Bayer, R. S. Cook, W. C. von Meyer, U. S. Patent 3, 821, 376, June 28, **1974**.
- [21] G. A. van Albada, R. C. G. G. Haasnoot, M. Lutz, A. L. Spek, J. Reedijk, *Eur. J. Inorg. Chem.* **2000**, 121–126.
- [22] A. Boultif, D. Louer, *J. Appl. Crystallogr.* **2004**, 37, 724–731.
- [23] Agilent, *CrysAlis PRO*. Agilent Technologies Ltd, **2014**, Yarnton, Oxfordshire, England.
- [24] G. M. Sheldrick, *Acta Crystallogr., Sect. A* **2015**, 71, 3–8.
- [25] Bruker, **2012**, Bruker AXS Inc., Madison, Wisconsin, USA.
- [26] O. V. Dolomanov, L. J. Bourhis, R. J. Gildea, J. A. K. Howard, H. Puschmann, *J. Appl. Crystallogr.* **2009**, 42, 339.
- [27] R. E. Marsh, V. Schomaker, F. H. Herstein, *Acta Crystallogr., Sect. B* **1998**, 54, 921–924.

Received: September 19, 2018

Self-Assembly

N. N. Adarsh, M. M. Dîrtu, P. Guionneau,
E. Devlin, Y. Sanakis, J. A. K. Howard,
B. Chattopadhyay, Y. Garcia* 1–8

**One-Dimensional Looped Chain and Two-Dimensional Square Grid Coordination Polymers: Encapsulation of Bis(1,2,4-Triazole)-*trans*-cyclohexane into the Voids**

The spontaneous self-assembly of bisazole ligands such as *m*-xylylenebis(tetrazole) (btzx), and bis(1,2,4-triazole)-*trans*-cyclohexane (btrcy) with $\text{Cu}(\text{NO}_3)_2$ and $\text{Cu}(\text{ClO}_4)_2$ resulted in a 1D looped chain (**1**) and a 2D square

grid (**2**), respectively. The grid architecture in **2** acts as an excellent host for the large guest ligand molecule btrcy, which was found encapsulated within the voids of the 2D coordination polymer.

DOI: 10.1002/ejic.201801138